



ELSEVIER

Journal of Nuclear Materials 266–269 (1999) 452–456

journal of  
nuclear  
materials

# Kinetic study of thermoelectric currents in the SOL plasmas

Oleg Batishchev <sup>\*,1</sup>, Brian LaBombard

*Plasma Science and Fusion Center, Massachusetts Institute of Technology, NW 16-258, 77 Massachusetts Avenue, Cambridge, MA 02139, USA*

## Abstract

The thermoelectric current instability in SOL plasma is one of the candidates to explain inner–outer plate asymmetries in tokamaks. This phenomenon is usually treated in the fluid approximation based on short mean free path assumptions, which may be violated for typical SOL plasma conditions. We applied a one-dimensional in space and two-dimensional in velocity Fokker–Planck code to study the problem assuming a uniform heat source and the absence of radiation. Kinetic simulation shows that although there does exist a collisionality range in which only asymmetric temperature solutions exist, the magnitude of the standard asymmetry is smaller than obtained from a fluid description and the corresponding thermoelectric currents in the SOL are suppressed. © 1999 Elsevier Science B.V. All rights reserved.

*Keywords:* SOL modeling; Kinetic theory

## 1. Introduction

There is experimental evidence of inner–outer plate asymmetries in the divertor region of tokamaks [1–3]. Observations include asymmetries in temperatures of the plasma, radiated energies, and heat fluxes to the plates. There are several possible candidates to explain these asymmetries:  $E \times B$  effects, neutrals recycling, radiation [4,5], and others. However, the simplest explanation may be based on the fact that when the temperature is different at the inner and outer plates, a thermoelectric current may be generated [6,7]. This current may significantly modify the amount of heat transmitted through the Child–Langmuir sheaths in front of the plates. The SOL plasma may therefore seek an asymmetric temperature profile in order to satisfy the boundary conditions.

With few exceptions [8], thermoelectric current effects have been studied using Maxwellian sheaths in combination with a short mean free path approximation for

electron transport. Ion transport has usually been neglected. Sheath transmission coefficients have been based on the assumption of a Maxwellian distribution of electrons. Under these conditions it has been shown that thermoelectric current may be large, and that it may cause up to 1:10 inner–outer asymmetries in the SOL with realistic parameters [9]. As it was shown before, kinetic effects may play an important role in the SOL plasma dynamics. They are responsible for flux-limiting, enhanced transport, and modified sheath conditions [10–12]. The intention of the current work is to study the thermoelectric current instability in the SOL using kinetic simulations.

## 2. Fluid model

We consider a one-dimensional ( $x$ ) plasma column bounded by two divertor plates at  $x = 0$  and at  $x = L$ . This is a reasonable approximation, because we are looking for a ‘simplest’ possible explanation [thermoelectric currents are predominantly parallel, 1D] of the inner–outer divertor asymmetries without bringing into the picture more complex effects related to the actual 3D geometry of the divertors.

Although oblique magnetic field was pointed out to be important [13], we neglect this effect in our model, because

<sup>\*</sup> Corresponding author. Tel.: +1 617 253 5799; fax: +1 617 253 0448; e-mail: oleg@psfc.mit.edu

<sup>1</sup> Also at Lodestar Research Corporation, Boulder, USA, Moscow Physical-Technical Institute and Keldysh Institute for Applied Mathematics, Moscow, Russian Federation.

our simulation is 1D in space and the divertor asymmetries occur in the open divertor configurations as well.

The fluid model is based on the Braginskii [14] plasma fluid limit for combined parallel electron and ion heat flux  $q_x$

$$q_x = eM(M^2 + 5)n_p T_p C_s - \kappa_x \nabla_x T_p - 3.21 T_p J_x, \quad (1)$$

with the assumptions that plasma species are equilibrated and that the distribution functions are Maxwellian in the zero order. Since  $J_x$  is approximately constant along the magnetic line, then even for initially symmetrical profiles any small asymmetric seed current (e.g. due to loop voltage) will result in the increased heat flux coming to one plate relative to the other. This will give a difference in plasma temperature at the plates, and consequently will give rise to an increase of the potential difference, and thus, an increase of the net current driven through the plasma.

The equilibrium solution for the  $q_x$  in front of the sheath must be equal to the heat flux allowed through the sheath,  $q_{sh}$  [15] (we assume no secondary emission).

$$q_x = q_{sh} \approx T_p \left\{ 4.49 + \ln[\mu^{0.5}/(1 - J_x/en_p C_s)] \right\} en_p C_s - J_x. \quad (2)$$

A step increase of  $J_x$  facilitates the solution of this equation by using a shooting method. What is important here is that it predicts a thermoelectric current driven bifurcation of plasma profiles. More details on fluid model may be found in the work [16].

### 3. Kinetic model

The plasma is described by two nonlinear kinetic equations for the time-dependent electron,  $f_e$ , and ion,  $f_i$ , distribution functions, which are strongly coupled by Coulomb collisions, self-consistent electric field, and neutral divertor recycling:

$$\frac{\partial f_e}{\partial t} = L_e + C_{ee} + C_{ei} + S_e + H_e, \quad (3)$$

$$\frac{\partial f_i}{\partial t} = L_i + C_{ii} + S_i + H_i, \quad (4)$$

where  $\mu = v_x/v$  is cosine of pitch angle,  $v = (v_x^2 + v_\perp^2)^{0.5}$  is modulus of velocity ( $x$  and  $v_x$  are parallel to the magnetic line);  $C_{ee}$ ,  $C_{ei}$ ,  $C_{ii}$  are corresponding Coulomb collision terms,  $S_e$  and  $S_i$  are volumetric mass sources,  $H_e$  and  $H_i$  are the volumetric energy source for electron and ion species, respectively.  $L_e$  and  $L_i$  combine free-streaming and electric field terms which can be written as

$$L_x = -v\mu \frac{\partial f_x}{\partial x} - \frac{1}{v^2} \frac{\partial}{\partial v} \left( v^2 \mu \frac{q_x E_x}{m_x} f_x \right) - \frac{1}{v} \frac{\partial}{\partial \mu} \left[ (1 - \mu^2) \frac{q_x E_x}{m_x} f_x \right], \quad (5)$$

where  $\alpha = e, i$ ;  $m_x$  and  $q_x$  are particle's mass and charge.

To study nonlinear effects in the parallel currents we have to take the Coulomb term  $C_{\alpha\beta}$  in its full form [16] (using Rosenbluth potentials,  $\nabla^2 \nabla^2 \psi^\beta = \nabla^2 \varphi^\beta = f^\beta$ ).

The imposed boundary conditions are modified logical boundary conditions [17], which account for net current  $J_x$  and enable self-consistently, the calculation of sheath potentials  $\Delta\Phi_{SH}^{in}$  and  $\Delta\Phi_{SH}^{out}$ :

$$\int_{-1}^0 \int_0^\infty v^3 \mu f_i - (x=0) dv d\mu - \int_{-1}^0 \int_0^{v_f^{in}} v^3 \mu f_e - (x=0) dv d\mu = -J_x, \quad (6)$$

$$\int_0^1 \int_0^\infty v^3 \mu f_i - (x=L) dv d\mu - \int_0^1 \int_0^{v_f^{out}} v^3 \mu f_e - (x=L) dv d\mu = J_x, \quad (7)$$

where  $v_f^{in,out} = -\sqrt{2e \Delta\Phi_{SH}^{in,out}/m_e}$ .

The steady-state, self-consistent parallel electric field  $E_x$  balances the ion and electron pressure gradients and the Coulomb electron–ion and plasma–neutral (e.g. due to ionization) friction forces

$$E_x = \{e(n_e/m_e + n_i/m_i)\}^{-1} \left[ \int \int (v^3 \mu (2C_{ei} + C_{eN} - C_{iN}) + (f_i - f_e)_x v^2 \mu^2) dv d\mu \right] \quad (8)$$

with a quasi-neutrality constraint  $n_e = n_i$ .

We adopt a simplified model for neutral recycling. Loss of mass to the walls is compensated by two ‘ionization’ sources attached to the plates:

$$S_i^{in} = S_e^{in} = S_0^{in} \exp(-x/\lambda^{in}), \quad (9)$$

$$S_i^{out} = S_e^{out} = S_0^{out} \exp(-(L-x)/\lambda^{out}), \quad (10)$$

provided  $(d/dt) \int_0^L S_i^{in,out} dx = \gamma^{in,out}$ , where  $\gamma^{in}$  in particle flux onto inner–outer plate, to keep mean density of plasma fixed.

The heating terms  $H_x$  in Eq. (3) and (4) are spatially localized sources (on interval  $L_h$ ) of prescribed power  $W_x$  deposited diffusively into the perpendicular component of velocity. This model was implemented in the Fokker–Planck code ALLA [18].

### 4. Numerical method

Our numerical approach combines splitting, velocity mesh with variable resolution, and a cubic spline technique with adaptive spatial step for the free-streaming term. A key feature is the usage of an operator splitting scheme with adaptive time step  $\tau$ , and an adaptive subdivision of the fractional time step  $\delta\tau$ . For instance, for

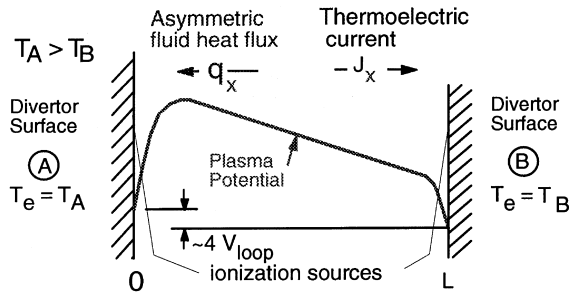


Fig. 1. Outside–inside electron temperature and density ratios as measured by probes plotted versus plasma collisionality. Kinetic modeling results are shown too.

the Coulomb collisions the sub-step is chosen locally, depending on the actual spatially varying collisionality  $\nu \propto n(t, x)/T^{1.5}(t, x)$ . This facilitates easy addition/exclusion of new terms in the equations, achieves conservation appropriate for a given fractional step, and enables accurate calculation of some functions needed for the electric field and sheath potential. In space, the grid is non-uniform and adaptive. The adaptive scheme de-

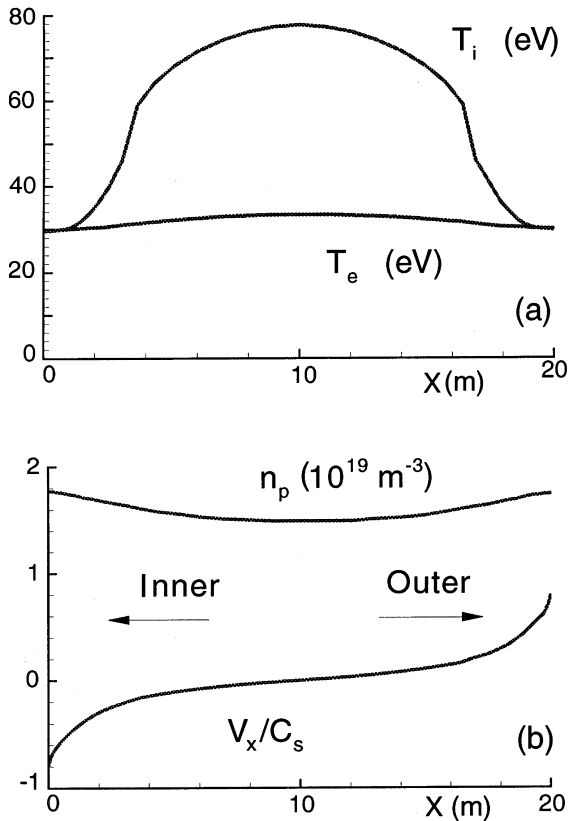


Fig. 2. Electron and ion temperatures, plasma density, and mean drift velocity in the low collisional case.

scription may be found in Ref. [19]. The velocity mesh is spherical axisymmetric  $v, \mu$ . The unknowns are cell-centered. Cell's center coordinates are  $v_i > 0$ ,  $\Delta v_i \equiv v_{i+1} - v_i = c \Delta v_{i-1}, i > 2, c \geq 1$ . The angular  $\mu$ -grid is non-uniform, though it corresponds to a uniform azimuthal mesh. Cell boundaries are chosen to give second order accurate evaluation of collisional fluxes.

We start from initially Maxwellian distributions of plasma with isobaric pure heat conduction profiles ( $T_p \propto x^{2/7}, n_p T_p = \text{const.}$ ) with small seed current  $J_x^0$  on the order of  $10^{-6} en_p^M C_s^M$ . We then calculate electric fields from Eq. (8), and sheath potentials from Eqs. (6) and (7). Next we solve Eqs. (3) and (4), find new distribution functions, and then repeated the procedure until a quasi-steady-state is achieved.

### 5. Results of the kinetic modeling

We adopted the following approximate C-Mod parameters: average  $n_p = 0.3\text{--}3 \times 10^{20} \text{ m}^{-3}$ ,  $T_e^M \approx 20\text{--}40 \text{ eV}$ ,  $L = 20 \text{ m}$ ,  $W \approx 30 \text{ MWt/m}^2$ ;  $m_i/m_e \approx 3680$ ;  $L_h = 12 \text{ m}$ ;  $\lambda^{\text{in}} = \lambda^{\text{out}} = 2 \text{ m}$ . Physical simulation time was about 1 ms (less for low collisional cases).

A general observation is that thermoelectric currents were generated when the collisionality  $\gamma$  was in the interval 0.01–0.4. However, the maximum value of  $J_x$  never grew higher than  $2 \times 10^{-2} n_p^D T_p^D$ . The maximum

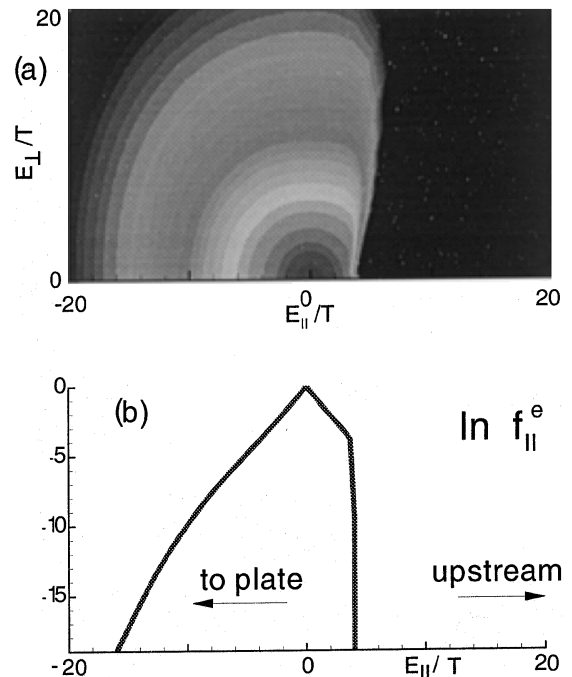


Fig. 3. (a) Electron distribution function at the divertor in the low collisional case plotted versus normalized parallel and perpendicular energies, (b) 1D cut at  $E_{\perp} = 0$ .

was achieved for  $\gamma$  around 0.03. The maximum ‘loop’ voltage was on the order of 0.4 V. The inner and outer divertor plates temperatures and the density variation are presented in Fig. 1. As can be seen, they are on the order of 0.5. Electron and ion temperature profiles for the case  $\gamma \approx 0.2$  are shown in Fig. 2(a). One can see that  $T_i$  significantly differs from  $T_e$  at the midplane. The density difference at the plates [Fig. 2(b)] is also small. The maximum Mach number of the flow (which appears to be symmetrical too) is about 0.75. The electron distribution function at the ‘inner’ plate is shown in Fig. 3(a). [Fig. 3(b) shows its cut at  $v_{\perp} = 0$ .] As one can see, the distribution is squeezed in  $v_x$ , and has a depleted tail at higher energies  $E$ .

Interestingly, the sheath potential value is about  $3.5 T_p$ . It was also found that the actual heat conductivity ratio to the classical Spitzer–Harm value varied in the 0.2–0.5 range (smaller than at the midplane), and the thermal force coefficient was on the order of 0.4 (instead of 0.71). Profiles of electron and ion temperatures became closer when collisionality increased (see Fig. 4(a) with  $\gamma = 0.02$  case). There is about a 20% difference in divertor temperatures and densities.

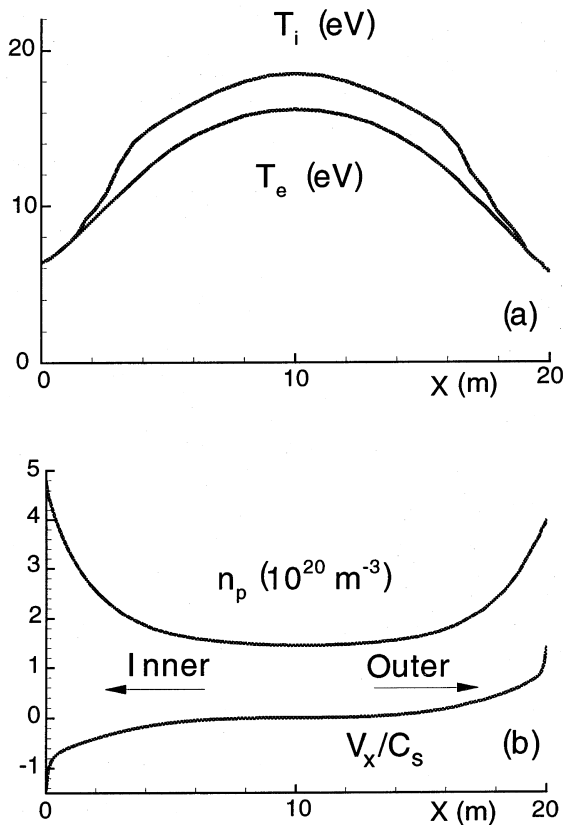


Fig. 4. Plasma temperature, density, and normalized mean velocity profiles for the collisional case.

As can be seen from Fig. 4(b), plasma flow becomes supersonic near the plates,  $M \approx 1.4$ . The electron distribution function becomes less elongated. However, there is a tail at high  $E$ , and the sheath potential rises to  $4.2 T_p$  [see Fig. 5(a) and (b)]. In this case, the heat conduction coefficient exceeded by a factor of 3 the short m.f.p. value near the plate (0.3 at the midplane), and thermal force coefficient rises to 0.5–0.6.

### 6. Conclusion

We have constructed a kinetic model to study thermoelectric currents in the divertor tokamaks. The model includes both electron and ion species dynamics in the presence of nonlinear Coulomb collisions, self-consistent parallel electric field and currents, and self-consistent Child–Langmuir sheaths. However, we adopted few simplifications. Important plasma radiation is neglected in our model. The heat source is assumed to be spatially uniform. Ionization is taken in a form of plasma source with fixed shape. Obviously, in our 1D2V model we are missing all two-dimensional effects.

Our simulations showed, that thermoelectric currents of the order of 1% of saturation current may be induced in the SOLs with collisionality  $\gamma$  in range 0.01–0.2 (peaked at 0.03). However, the observed temperature and density inner–outer variation was on the order of

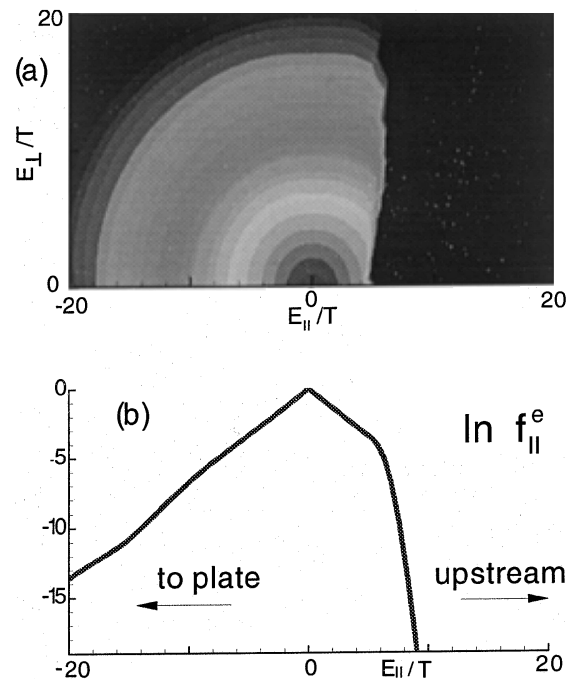


Fig. 5. (a) Electron distribution function at the divertor in the collisional case plotted versus normalized parallel and perpendicular energies, (b) 1D cut at  $E_{\perp} = 0$ .

50%, which is much smaller than the experimental observations. The following kinetic corrections, found in our simulation may affect fluid models: (i) enhanced sheath potential ( $3.5\text{--}4.2 T_p$ ), (ii) modified sheath energy transmission coefficient, (iii) flux-limiting in the upstream and enhanced conductivity near the plates, (iv) reduced thermal force coefficient, (v) difference in electron and ion temperatures, (vi) Mach number may differ from 1 near the plates.

In our future research, we will improve the neutral ionization model and will account for radiation, because it seems that thermoelectric effects cannot be solely responsible for the inner–outer plates asymmetries in the SOL plasma.

#### Acknowledgements

This work is supported by US Department of Energy Contracts No. DE-FG02-97-ER-54392 at Lodestar Research Corporation, and DE-AC02-78-ET-5103 and DE-FG02-91-ER-54109 at MIT PSFC.

#### References

- [1] A.V. Chankin et al., *J. Nucl. Mater.* 196–198 (1992) 739.
- [2] K. Itami et al., *J. Nucl. Mater.* 196–198 (1992) 757.
- [3] B. LaBombard et al., *J. Nucl. Mater.* 241–243 (1997) 149.
- [4] M.J. Shaffer, B.J. Leikind, *Nucl. Fusion* 31 (1991) 1740.
- [5] G.M. Stabler, *Nucl. Fusion* 38 (1996) 1437.
- [6] P.J. Harbour, *Contr. Plasma Phys.* 28 (1988) 417.
- [7] P.J. Harbour et al., *J. Nucl. Mater.* 162–164 (1988) 236.
- [8] M.G. Haines, *Contr. Plasma Phys.* 38 (1998) 343.
- [9] B. LaBombard et al., *Bull. Am. Phys. Soc.* 41 (1996) 1481.
- [10] K. Kupfer et al., *Phys. Plasmas* 3 (1996) 3644.
- [11] O.V. Batishchev et al., *Phys. Plasmas* 4 (1997) 1672.
- [12] O.V. Batishchev et al., *J. Nucl. Mater.* 241–243 (1997) 374.
- [13] M. Shimada, T. Ohkawa, these Proceedings.
- [14] S.I. Braginskii, *Reviews Plasma Physics*, vol. 1, Consult. Bureau, New York, 1965, p. 205.
- [15] P.C. Stangeby, *Phys. Fluids* 27 (1984) 682.
- [16] B. LaBombard, Fluid model of thermoelectric currents in the SOL, to be published in *Phys. Plasmas*.
- [17] R.J. Procassini et al., *Nucl. Fusion* 30 (1990) 2329.
- [18] A.A. Batishcheva et al., *Phys. Plasmas* 3 (1996) 1634.
- [19] O.V. Batishchev, *Contr. Plasma Phys.* 38 (1998) 213.